

## RWM feedback stabilization in DIII-D: experiment-theory comparisons and implications for ITER

A.M. Garofalo,<sup>1</sup> J. Bialek,<sup>1</sup> M.S. Chance,<sup>2</sup> M.S. Chu,<sup>3</sup> D.H. Edgell,<sup>4</sup> G.L. Jackson,<sup>3</sup>  
T.H. Jensen,<sup>3</sup> R.J. La Haye,<sup>3</sup> G.A. Navratil,<sup>1</sup> M. Okabayashi,<sup>2</sup> H. Reimerdes,<sup>1</sup>  
J.T. Scoville,<sup>3</sup> and E.J. Strait<sup>3</sup>

<sup>1</sup>*Columbia University, New York, NY 10027, USA*

<sup>2</sup>*Princeton Plasma Physics Laboratory, P.O. Box 451, Princeton, NJ 08543 USA*

<sup>3</sup>*General Atomics, P.O. Box 85608, San Diego, CA 92186, USA*

<sup>4</sup>*Far-Tech, Inc., San Diego, CA 92121, USA*

Plasma operation with high values of  $\beta_N$  and of the bootstrap current fraction in the advanced tokamak requires stabilization of the low toroidal mode number  $n$  ideal magnetohydrodynamic (MHD) kink mode. In the presence of a nearby resistive wall, the kink becomes a slowly growing resistive wall mode (RWM). Recent experiments in DIII-D have demonstrated sustained RWM stabilization by plasma rotation achieved with improved error field correction and sufficient angular momentum injection [1]. The experimental data from DIII-D is so far consistent with the RWM calculations by Bondeson and Ward [2]. The agreement between the predicted and measured rotation velocity threshold is within a factor of two [3]. However, until the quantitative understanding of the stabilization mechanism is improved, it is not possible to extrapolate with confidence the rotation velocity threshold for RWM stabilization to ITER or reactor plasmas. Furthermore, in the fusion-reactor regime, lacking the large external torque of present neutral beam-driven tokamaks, the rate of rotation needed for RWM stability may not be achieved.

Conversely, active feedback stabilization of the RWM via magnetic coils is predicted to allow stable  $\beta_N$  values up to near the limit allowed by a perfectly conducting wall, the ideal-wall limit, even in absence of plasma rotation [4]. Direct feedback stabilization of the RWM, i.e., with toroidal plasma rotation below the critical value for RWM stability, has been observed in DIII-D experiments. This result, obtained both using the external coil set (C-coil) and the newly installed internal coil set (I-coil), is in agreement with the results of feedback simulations.

DIII-D studies of the RWM feedback stabilization process, in absence of significant plasma rotation, have pursued two approaches: (1) reduce the toroidal plasma rotation, and (2) increase the plasma rotation threshold for RWM stabilization. The plasma rotation can be reduced in several ways: using low-torque neutral beams (the nearly perpendicular "right" sources in DIII-D), and/or using magnetic braking.

With reduced neutral-beam torque, the slower rotating plasma exhibited an unstable RWM, which was stabilized by C-coil feedback with no change in toroidal rotation as shown in Fig. 1. The reference discharge is a "fast  $I_p$  ramp" plasma in which the RWM

occurred reproducibly at  $t \sim 1800$  ms, even at relatively low beta, suggesting that its onset was driven at least in part by the evolution of the safety factor profile. A slightly de-optimized correction of the  $n = 1$  error field is used in order to slow down the plasma rotation. The feedback field is applied using the external control coil, the C-coil, in response to the  $n = 1$  signal from internal poloidal field sensors. Figure 1 shows the results of a scan of the feedback gain: the RWM became more unstable (stronger effect on the plasma) with decreasing feedback gain. There was no discernible effect of the feedback field on the plasma rotation before the RWM onset. This suggests that the plasma relies primarily on the feedback system for its stability.

In another experiment, strong magnetic braking reduced the plasma rotation to essentially zero over most of the plasma. With I-coil feedback control, this discharge survived for more than 100 ms at beta above the no-wall stability limit (approximated by  $2.1 \times \ell_i$ ) after the rotation is reduced, until one of the feedback power supplies trips out [5].

A similar discharge without feedback becomes unstable earlier, despite higher rotation and lower beta, as shown in Fig. 2. The braking field is an  $n = 1$  field applied by the feedback itself, due to an offset in the sensor signals. The results of this feedback experiment using internal control coils and poloidal field sensors are compared to calculations carried out with an analytic, ideal MHD feedback model in slab geometry. The model has been previously used successfully to predict the dynamics of the DIII-D RWM feedback system using the external control coil set (C-coil) and radial field sensors [6].

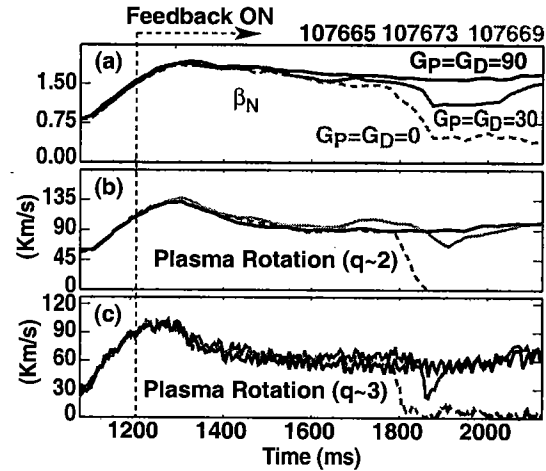


Fig. 1. Low rotation plasma target for RWM feedback studies produced using mostly perpendicular neutral beam sources. (a) Feedback gain scan and its effect on  $\beta_N$ . (b,c) Absence of correlation between feedback gain and plasma rotation suggests direct feedback stabilization of the RWM.

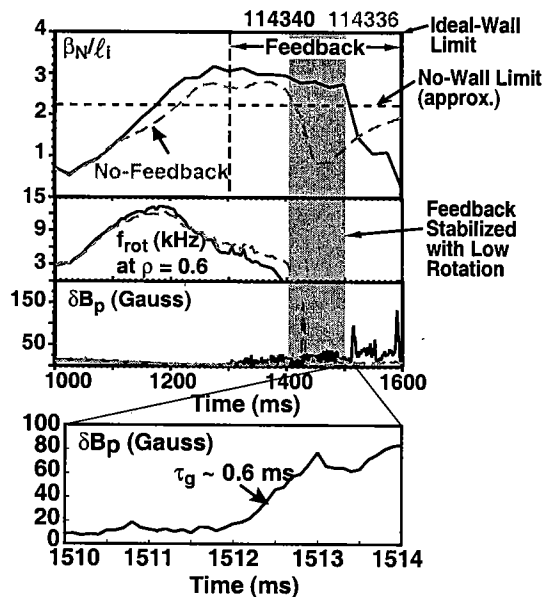


Fig. 2. Low rotation plasma targets produced using  $n = 1$  magnetic braking. (a) Discharge with RWM feedback lasts  $\sim 100$  ms with  $\beta_N$  above the no-wall limit of  $2.1 \times \ell_i$  even after the (b) plasma toroidal rotation drops to zero. (c) Mirnov loop  $n = 1$  amplitude showing RWM onset, and (d) expanded view to show the RWM growth time measured when the feedback system fails. Comparison discharge without feedback (dashed lines) becomes unstable even at lower beta, as the plasma rotation approaches zero.

The model uses the assumption that only one mode is involved; therefore, the plasma response is given by only one parameter (e.g., the instability strength). It is assumed that the vector potential  $\bar{a}$  of the field perturbation  $\bar{b} = \nabla \times \bar{a}$  is of the form:

$$\bar{a}(x, y, z, t) = \left( \hat{z} - \frac{k_p}{k_t} \hat{y} \right) e^{i(k_t y + k_p z)} \varphi(x, t) . \quad (1)$$

The  $x$ -direction is the radial direction, away from the plasma, and  $x = 0$  is the position of the resistive wall. The  $y$ -direction is the toroidal direction, and the wave number in this direction is  $k_t = n/R$ , with  $R$  the major radius of the tokamak at the outboard wall. The  $z$ -direction is the poloidal direction, and  $k_p = m/r$  is the wave number in this direction, with  $r$  the minor radius of the tokamak vessel wall. If the feedback current is a current sheet located at  $x = b$  ( $\geq 0$ ), we can use the assumption in Ref. 6 that the perturbed plasma current (a sheet current located at  $x = -r$ ) is proportional to the perturbed vector potential at the wall.

The actual closed-loop gain of the DIII-D feedback system can be represented by the expression:

$$G(i\omega) = \frac{1}{1 + i\omega \tau_p} \left( g_p + \frac{g_D i\omega \tau_D}{1 + i\omega \tau_D} \right) \times \frac{\Omega_{U1}}{\Omega_{U1} + i\omega} \times \frac{\Omega_{U2}}{\Omega_{U2} + i\omega} . \quad (2)$$

Here, the symbols  $g_p$  and  $g_D$  denote the proportional and derivative gain, respectively. The first low pass filter with upper cutoff frequency  $1/\tau_p$  is used to reduce noise in the sensors. The derivative gain is implemented as a high pass filter with lower cut-off frequency  $1/\tau_D$ . The last two low pass filters represent the transfer function of the controller+amplifier+coil chain. The upper cutoffs  $\Omega_{U1}$  and  $\Omega_{U2}$  are free parameters determined by a fit to measurements of the open-loop transfer function.

For a ‘‘Smart Shell’’ feedback, with sensors measuring the flux at the resistive wall,  $\varphi(0, t)$ , the feedback current is obtained from

$$J_F = -G(i\omega)\varphi/M , \quad (3)$$

where  $M = \mu_0 e^{-kb} / 2k$  is the mutual inductance, and  $k = \sqrt{k_t^2 + k_p^2}$ . The dispersion relation for this feedback scheme was shown in Ref. 6 to be:  $\alpha - i\omega\tau - G(i\omega) = 0$ , with  $\tau$  the resistive wall time, and  $\alpha$  the plasma stability parameter ( $\alpha/\tau$  is the RWM growth rate without feedback).

If the sensors are assumed to measure the poloidal field at the resistive wall,  $b_z = -(k_p/k_t) [\partial\varphi(x, t)/\partial x]_{x=0^-}$ , we can write the coupling between the poloidal field sensors and the control coils as  $M' = -kM(k_p/k_t)$ , and the feedback current is:

$$J_F(t) = -\frac{G(i\omega)}{M'} \left[ -\frac{k_p}{k_t} \frac{\partial\varphi(x, t)}{\partial x} \right]_{x=0^-} = (1 + 2\alpha) \frac{G(i\omega)}{M} \varphi(0, t) . \quad (4)$$

The dispersion relation becomes:

$$\alpha - i\omega\tau + (1 + 2\alpha)G(i\omega) = 0 \quad (5)$$

Equation (5) describes a feedback algorithm using strongly coupled poloidal field sensors and feedback coils. In the DIII-D experiment, the poloidal field sensors and the feedback coils are nearly completely decoupled. The algorithm, “Mode Control” feedback, can be simulated by subtracting from the input to the feedback controller the coupling between sensors and feedback coils. The dispersion relation becomes:

$$\alpha - i\omega\tau + \frac{(1 + 2\alpha)G(i\omega)}{1 - G(i\omega)/(1 + i\omega\tau)} = 0. \quad (6)$$

The marginally stable solutions to the dispersion relation in Eq. (6), are shown in Fig. 3 by the associated values of  $g_p$  as a function of the open-loop growth time. The strongest RWM that can be stabilized by the feedback system used in the experiment shown in Fig. 2, corresponds to an open-loop RWM growth time  $\tau_g \approx 1.1$  ms. This calculation is consistent with the experiment, where the measured RWM growth time soon after the feedback fails is  $\tau_g \approx 0.6$ . Modeling indicates that the feedback performance would be improved by reducing the feedback gain and also by increasing the upper cutoff frequency of the digital filter (smaller  $\tau_p$ ).

The equations of the model are easily adapted to simulate other control algorithms, coil-sensor configurations, and power supplies characteristics. Of particular interest for the design of RWM feedback stabilization in ITER, are the results for a feedback system using internal control coils with poloidal field sensors. It can be readily shown how this choice of sensors and coils allows the system to stabilize a mode with growth rate exceeding the “speed” of the system itself, i.e., the upper cutoff frequency of the open loop transfer function.

## References

- [1] A. M. Garofalo, T.H. Jensen, L.C. Johnson, *et al.*, Phys. Plasmas **9**, 1997 (2002).
- [2] A. Bondeson and D.J. Ward, Phys. Rev. Lett. **72**, 2709 (1994).
- [3] R.J. La Haye, submitted to Nucl. Fusion (2004).
- [4] J. Bialek, A.H. Boozer, M.E. Mauel, *et al.*, Phys. Plasmas **8**, 21709 (2001).
- [5] E.J. Strait, J. Bialek, N. Bogatu, *et al.*, Phys. Plasmas **11**, 2505 (2004).
- [6] A.M. Garofalo, T.H. Jensen, and E.J. Strait, Phys. Plasmas **9**, 4573 (2002).

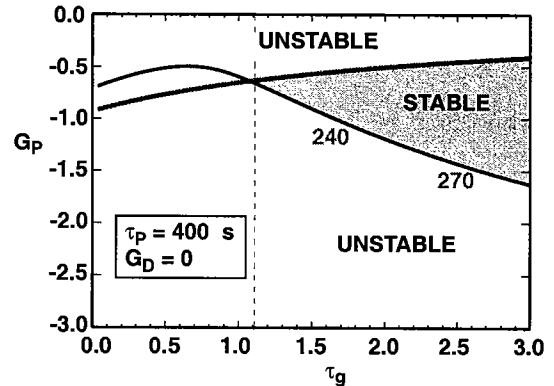


Fig. 3. Marginal stability boundaries for the RWM feedback system with settings used in discharge 114340. Numbers along the boundaries are the real frequency of the mode in Hz. The feedback gain has to be in the shaded area to allow system stability. Strongest RWM that can be stabilized in this case has growth time  $\sim 1.1$  ms.